



7<sup>th</sup> International Conference on Fatigue Design, Fatigue Design 2017, 29-30 November 2017, Senlis, France

## Experimental monitoring of the self-heating properties of thermoplastic composite materials

Laura Muller<sup>a\*</sup>, Jean-Michel Roche<sup>a</sup>, Antoine Hurmane<sup>a</sup>, Didier Pacou<sup>a</sup>, Vincent Bonnard<sup>a</sup>, Catherine Peyrac<sup>b</sup>, Laurent Gornet<sup>c</sup>

<sup>a</sup>ONERA, The French Aerospace Lab, F-92322 Châtillon, France

<sup>b</sup>CETIM, 52 avenue Félix Louat, 60300 Senlis, France

<sup>c</sup>Ecole Centrale de Nantes, 1 rue de la Noë, 44321 Nantes, France

---

### Abstract

The full estimation of the fatigue lifetime of a given material is needed for the industrial structures sizing. However, it requires time-consuming, expensive fatigue testing campaigns and a huge number of samples. An alternative experimental procedure is based on the monitoring of the “self-heating” properties. The aim here is to correlate the fatigue limit with a change of thermal behavior. The main advantage of such tests is that they only require few samples and are constituted of a limited number of mechanical cycles. Thus, self-heating tests lead to an accelerated estimation of the endurance limit. The purpose of the present paper is to validate this approach for carbon/thermoplastic composite materials.

© 2018 The Authors. Published by Elsevier Ltd.

Peer-review under responsibility of the scientific committee of the 7th International Conference on Fatigue Design.

*Keywords:* endurance limit ; self-heating ; thermal behavior ; carbon/thermoplastic composite

---

\* Corresponding author. Tel.: +33 1 46 73 45 28

*E-mail address:* [laura.muller@onera.fr](mailto:laura.muller@onera.fr)

## Nomenclature

$\sigma$ or $S$	stress (MPa)
$\sigma_{maxi}$	maximal stress of a given block of mechanical cycles (MPa)
$\sigma_D$	stress value corresponding to the end of the linear domain during tensile test (MPa)
$R_M$	fracture stress value in tensile test (MPa)
$N$	number of mechanical cycles to failure (-)
$\varepsilon_l$	longitudinal strain (-)
$\varepsilon_t$	transversal strain (-)
$R$	load ratio (-)
$T$	temperature (°C)
$\theta$	temperature rise or heating (°C)
$\theta_{exp}$	experimental temperature rise reached at the end of a block of mechanical cycles (°C)
$\theta_F$	stabilized temperature rise (°C)
$\tau$	characteristic time of the thermal drift during mechanical cycles (s)
$A_1$	amplitude of the first harmonic of the thermal signal (°C)
$\phi_1$	phase of the first harmonic of the thermal signal (rad)

## 1. Introduction

### 1.1. Composite materials

Composite materials are made of at least two components, usually fibers and matrix, which confer to the new material better mechanical properties than those of individual components [1], [2]. The fibers, either glass-fibers or carbon-fibers, confer the mechanical properties to the whole material, while the matrix is used as a resin to link the fibers to each other, and to distribute the loads applied on the material [3], [4]. Composite materials offer a strength/weight ratio better than the one of other homogeneous materials, like steel: this is why they are more and more used in aerospace industry [5]. The structure of composite materials depends on the orientation, the architecture and the size of the fibers, which can be short or continuous. Continuous fibers might be aligned in one preferential direction (unidirectional) or might be woven according to two or three directions.

### 1.2. Fatigue of composite materials

The fatigue phenomenon appears during the lifetime of a structure under cyclic loading. Indeed, during cyclic loading, the material might break even if the maximal load is lower than the damage threshold (thus lower than the failure load). A common way to represent fatigue behavior is to use the Wöhler or S/N curves which provide the number of cycles to failure for each load level [6], [7].

In order to build the Wöhler curve of a given material, a large number of mechanical tests are required. A cyclic load can be defined by its frequency, mean and maximal (or minimal) loads and the load ratio (ratio between maximal and minimal load). For a given cyclic load, the sample is tested until it breaks, and the number of cycles to failure  $N$  is reported on the curve. The process is repeated for each load  $S$ , from the lowest ones to the failure one (fracture load  $R_M$ ). For the lowest loads, the sample can be tested for weeks before failure, or never break at all. (Fig. 1).

For many materials, an asymptote can be detected on the curve, for the lowest load values. Under this asymptote, the risk of a premature failure is almost non-existent: it seems that the sample would never break in fatigue. Such a limit, which is called the “fatigue limit”, is used for structure designing purposes in the industry. However, the main drawback of this strategy, based on the use of Wöhler curves, is that they are built after several months of mechanical tests, and require a large number of samples (at least 5 by load level to reduce the data scattering).

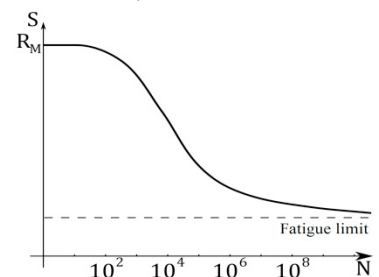


Fig. 1 : Wöhler curve

### 1.3. Self-heating tests

An alternative to the fatigue tests might be self-heating tests. These tests are also based on cyclic loads, but instead of cycling each sample to failure for several given load values, only a limited number of mechanical cycles are applied to one sample, for increasing load values (Fig. 2). During every block of cycles, the self-heating of the sample, which increases until it reaches a stabilized value, is recorded by thermocouples or an infrared camera. The self-heating is the temperature increment between the current temperature and the room temperature. As illustrated by Fig. 3, the evolution of the stabilized heating with the maximal stress value of each block enables to identify two tendencies: for the lowest load values, the stabilized heating is almost constant; then, after a specific load value, the heating strongly increases, which seems to indicate an alteration of the viscous properties of the resin and/or the initiation of fatigue damage.

Moreover, it has been proven for metallic materials [8]–[10] and some composite materials [5], [7], [11] that the load value from which the heating speeds up is linked to the fatigue limit determined from the Wöhler curves. (Fig. 3) It seems that the evolution of the fatigue damage might be monitored by change in thermal behavior of the material. Ultimately, the self-heating tests might even lead to an estimation of the fatigue limit of a material, much faster than with the standard fatigue tests, since the number of load cycles is much lower and only few samples are needed. Overall, the test duration will not exceed a few days, instead of the usual campaigns which last several months.

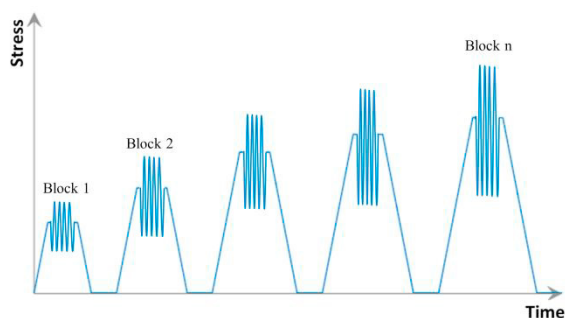


Fig. 2 : Schematic representation of self-heating tests

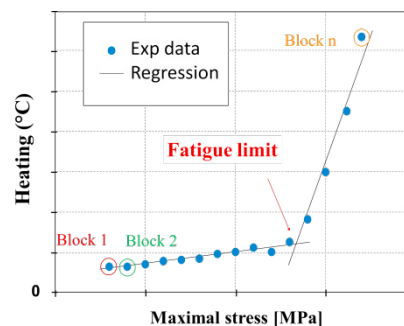


Fig. 3 : Self-heating curve

The purpose of this paper is to check if the self-heating evolutions described before for thermoset composites are still valid for thermoplastic composites, as already suggested in recent studies [12], [13]. Furthermore, the paper aims at comparing the thermal behaviors of the material under quasi-static tensile tests and under cyclic loading. Also, different approaches to analyze the change of thermal behavior are discussed, such as the estimation of the first harmonic of the thermal signal, which is made possible by a lock-in detection.

## 2. Material characterization with static tests

### 2.1. Experimental procedure

The studied material is a balanced plain woven carbon/PA66 thermoplastic composite, of a 2 mm thickness. Samples are rectangular ( $250 \times 25 \text{ mm}^2$ ), along three directions:  $0^\circ$ ,  $90^\circ$  and  $45^\circ$ . Three samples Static tests are carried out on a 150 kN ZWICK machine, equipped with mechanical grips, with a load speed of 2 MPa/s. The evolution of the displacement fields during the tests is monitored by Digital Image Correlation (DIC), with optical cameras of a 2 Mpx resolution. The acquisition frequency is 5 images per second. At the same time, the heating is monitored by a FLIR X6540sc mid-wave infrared camera, used on a  $[3\text{--}5] \mu\text{m}$  wavelength range, with a 20 mK thermal sensitivity and a space resolution of  $640 \times 512$  pixels. The acquisition frequency is 100 Hz. Two acoustic

sensors are also used to record each acoustic emission occurring during the test. In the present paper, acoustic data is not reported since it is still under post-processing.

2.2. Mechanical results

Three samples by orientation are tested up to failure. From measured displacement fields, the strain fields are calculated, which allows to assess the Young modulus and the Poisson’s ratio.

The Young modulus  $E$  is defined as the ratio between the stress  $\sigma$  and the longitudinal strain  $\epsilon_l$  (red curve in Fig. 4), in the elastic domain of the material. According to the EN 2561-95 norm, the Young modulus is experimentally determined by calculating the slope of  $\sigma(\epsilon_l)$  on a stress range between 10% and 50% of the yield stress. However, this norm applies for laminate (unidirectional) composite only. As there is no equivalent norm for woven composites, the same procedure is used to evaluate  $E$ , assuming that the material strength is large enough (black curve, Fig. 4).

The Poisson’s ratio is defined as the ratio between the transverse and the longitudinal deformation. Like for the Young modulus, the Poisson’s ratio is calculated on the  $\epsilon_t(\epsilon_l)$  curve between 10% and 50% of the yield stress.

Table 1 summarizes the properties for each orientation by averaging the values obtained for each sample.

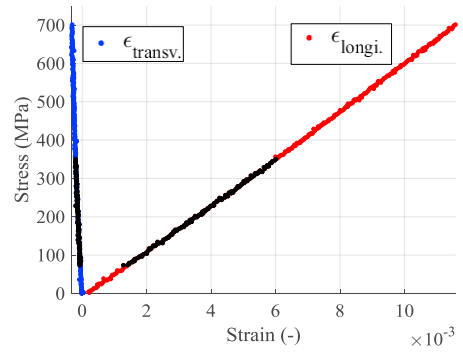


Fig. 4 : Stress-strain curve, with the longitudinal strain (red) and transversal strain (blue), and the domains used for the evaluation of the Young modulus and the Poisson’s ratio (black)

Table 1: Elastic properties and ultimate tensile stress of the studied carbon T700/PA66 thermoplastic composite material

Orientation	Ultimate tensile stress	Young modulus	Poisson’s ratio
0° (warp)	695 MPa	59 GPa	0.031
90° (weft)	595 MPa	58 GPa	0.033
45° (shear)	265 MPa		

2.3. Thermal results

The study of the thermal behavior of a sample during a static tensile test might give a quick approximation of the fatigue limit [14] under which the material is assumed not to be damaged by cyclic loads. The thermal behavior of a sample during a static test can indeed be divided in three domains:

- A first domain, in which the mechanical behavior is elastic. The temperature linearly decreases by thermoelastic effect.
- A second domain, in which the mechanical behavior is anelastic. The temperature evolution becomes non-linear and eventually gets stabilized to a minimum. Micrographic analyses show the appearance of micro damage.
- A third domain, in which damage propagates until the sample final failure. The temperature non-linearly increases due to local heat sources appearing with macroscale damage.

The stress value  $\sigma_D$  corresponding to the end of the linear domain of the heating has been compared and identified to the fatigue limit [14].

The evolution of the heating, averaged over the whole sample, is given in Fig. 5. The observed thermal behavior is in good agreement with the literature description, and the stress value  $\sigma_{Dii}$  in the orthotropic direction (i) can be estimated (red dot in Fig. 6) as the end of the thermoelastic domain. To estimate the stress value  $\sigma_D$ , a fitting of the experimental curve is performed with two linear regressions, beginning with few experimental data, and increasing the number of experimental data until all the experimental curve is considered.  $\sigma_D$  corresponds to the intersection between the two linear regressions which have the better correlative coefficient. Then, a bootstrap statistics

approach is used to randomly redistribute the experimental data, and calculate again the new intersection. The redistribution is applied several times (10 to 100 times the number of experimental data), and the several intersections are used to produce a confidence interval, bounded by percentiles 2,5 % and 97,5 % of the bootstrap distribution.

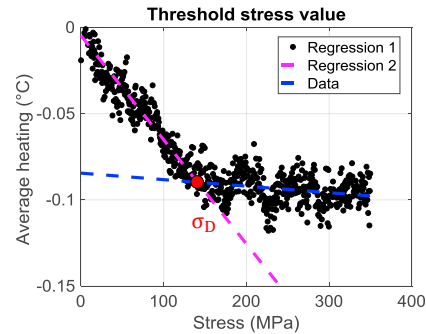
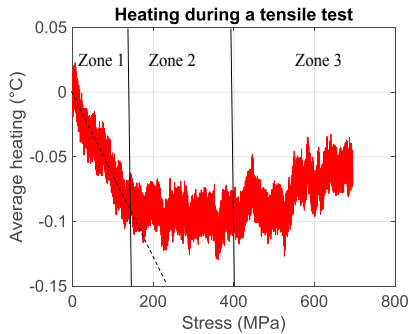


Fig. 5 : Spatial average heating of the sample during a static test

Fig. 6 : Estimation of stress value  $\sigma_D$  based on a bootstrap approach

Table 2 presents the values obtained in the cases of  $0^\circ$  and  $90^\circ$  samples. For the  $45^\circ$  samples, the cooling phenomenon is almost nonexistent because of major viscous effects, and the method will have to be adjusted to assess the shear fatigue limit  $\sigma_{D12}$ .

Table 2 : Stress value  $\sigma_D$  for the warp and weft orientations

Orientation	Stress value $\sigma_D$
$0^\circ$ (warp)	135 MPa
$90^\circ$ (weft)	130 MPa

The next step will be to estimate the load value for which the temperature is minimal. Since this value seems to match with the appearance of micro damage, it could be similar to the fatigue limit. Then, the aim will be to understand which phenomena (viscosity, damage) are involved in the variation of temperature, to finally see if it can be linked to a first estimation of the fatigue limit.

### 3. Self-heating tests campaign

#### 3.1. Experimental procedure

The self-heating tests, presented in Fig. 2, are carried out on a 100 kN-hydraulic machine, equipped with hydraulic cooled grips. The frequency of the cyclic load is 4.72 Hz in order to avoid any resonance effect between the frequency of the tests and of the infrared camera. The stress ratio is constant:  $R = 0.1$ . The tests are built with 12 blocks of cycles, 6,000 cycles per block. Displacement and thermal fields are respectively monitored by an optical camera dedicated to image correlation and an infrared camera (FLIR sc7000) similar to the ones used for the static mechanical tests. The acoustic activity is recorded with two acoustic sensors.

In the next two subsections, thermal results only are discussed. The digital image correlation and the acoustic emission data have not been analyzed yet.

#### 3.2. Theoretical approach of the self-heating of the composite under cyclic loading

During a cyclic mechanical loading, characterized by its pulsation  $\omega = 2\pi f$  (with  $f$  the frequency of the solicitation), the global thermal signal can be written as a Fourier decomposition (equation (1)):

$$T(t) = T_{drift}(t) + \sum_{n=1}^{\infty} a_n \cos(n\omega t) + \sum_{n=1}^{\infty} b_n \sin(n\omega t) \quad (1)$$

With  $a_n$  and  $b_n$  the Fourier coefficients.

In this study, only the first harmonic ( $n = 1$ ) is considered. It is more convenient to consider temperature rise that temperature itself :  $\theta(t) = T(t) - T(t_0)$ . Assuming  $A_n = \sqrt{a_n^2 + b_n^2}$  and  $\tan \phi_n = b_n/a_n$ , the harmonic can be defined by an amplitude  $A_1$  and a phase  $\phi_1$ , as shown in equation (2) :

$$\theta(t) = \theta_{drift}(t) + A_1 \cos(\omega t + \phi_1) \quad (2)$$

The first term of equation (2) can be seen as a thermal drift; the second one is the oscillating part locked-in to the mechanical frequency.

The thermal drift is governed by three types of thermal transfer: conduction, convection and radiation. In our case, the sample is assumed to be thin enough to have an homogeneous temperature within its volume, which means conduction in the material can be neglected. Since radiation is also considered negligible, only the convective effects influence the temperature of the sample. A thermal equilibrium of the sample leads to equation (3) :

$$\frac{\partial T(t)}{\partial t} = -\frac{2h}{\rho c_p e} (T(t) - T_{\infty}) \quad (3)$$

Where  $h$  is the coefficient of convection transfer ( $W m^{-2}K^{-1}$ ),  $\rho$  the density ( $kg m^{-3}$ ),  $c_p$  the thermal capacity of air ( $J kg^{-1}K^{-1}$ ),  $e$  the thickness of the sample ( $m$ ),  $T$  the temperature of the sample ( $^{\circ}C$ ) and  $T_{\infty}$  the ambient temperature ( $^{\circ}C$ ). If  $\frac{2h}{\rho c_p e} = \frac{1}{\tau}$ ,  $\tau$  being a characteristic time (s), the solution of (3) is given by equation (4) :

$$T(t) = T_{\infty} + K e^{-\frac{t}{\tau}} \quad (4)$$

$K$  is determined at  $t = 0$ , the temperature rise (or heating)  $\theta(t)$  is obtained by subtracting the initial temperature  $T(0)$  to the temperature of the sample  $T(t)$ , and the stabilized temperature rise (heating value  $\theta_F$ ) is defined as the subtraction between  $T_{\infty}$  and  $T(0)$ . The equation (5) summarizes the final expression of the first term of the equation (2):

$$\theta_{drift}(t) = \theta_F (1 - e^{-\frac{t}{\tau}}) \quad (5)$$

Experimentally, the thermal drift is fitted by  $\theta_{drift}$ , and the stabilized temperature rise is used as thermal indicator for each load level during the self-heating tests.

The oscillating part of the thermal signal corresponds to the first harmonic of the thermal signal, defined by its amplitude  $A_1$  and its phase  $\phi_1$ . This harmonic describes the thermoelastic behavior of the material.

### 3.3. Experimental passive thermal monitoring at low IR camera frequency acquisition

The first chosen approach is to monitor the heating of the sample with a low frequency acquisition of 1 image per second. Under these experimental conditions, only the thermal drift can be analyzed since no sinusoidal evolution can be found. As illustrated by Fig. 7, the stabilized temperature rise value  $\theta_F$  is indeed checked for a given load level. It is also checked that  $\theta_F$  tends to increase with the stress level, which is in good agreement with literature (Fig. 8).

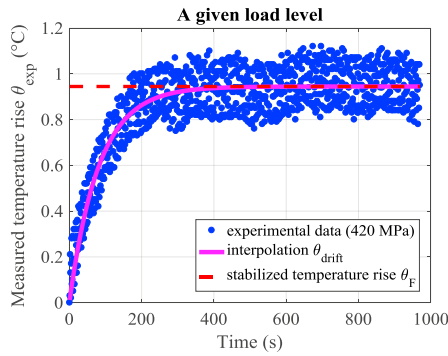


Fig. 7 : Measured self-heating  $\theta_{exp}$  for a given stress level and estimation of the stabilized temperature rise  $\theta_F$ . Thermal acquisition setup: 1 image per second. Composite at  $90^\circ$

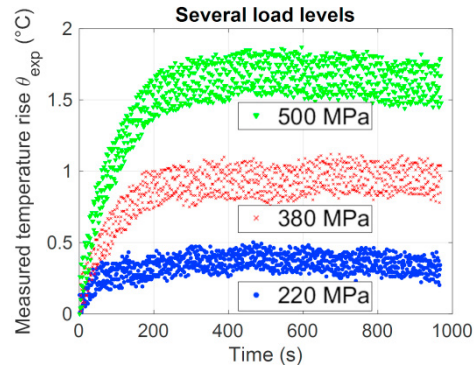


Fig. 8 : Variation of temperature rise between from one stress level to another. Composite at  $90^\circ$

The evolution of  $\theta_F$  with the maximal stress level on each step leads to build the “self-heating curves”. They are displayed in Fig. 9 for three specimens: one at  $0^\circ$  and two at  $90^\circ$ . The stake here is to identify a change of thermal behavior for a threshold stress value which will ultimately be compared to the fatigue limit, in order to verify if this thermal behavior change can be directly related to fatigue damage. The method used to identify the threshold value is the same as for tensile tests: the best intersection between two linear regressions is kept, for several redistributions of the experimental data, and the several intersection data calculated produce a confidence interval.

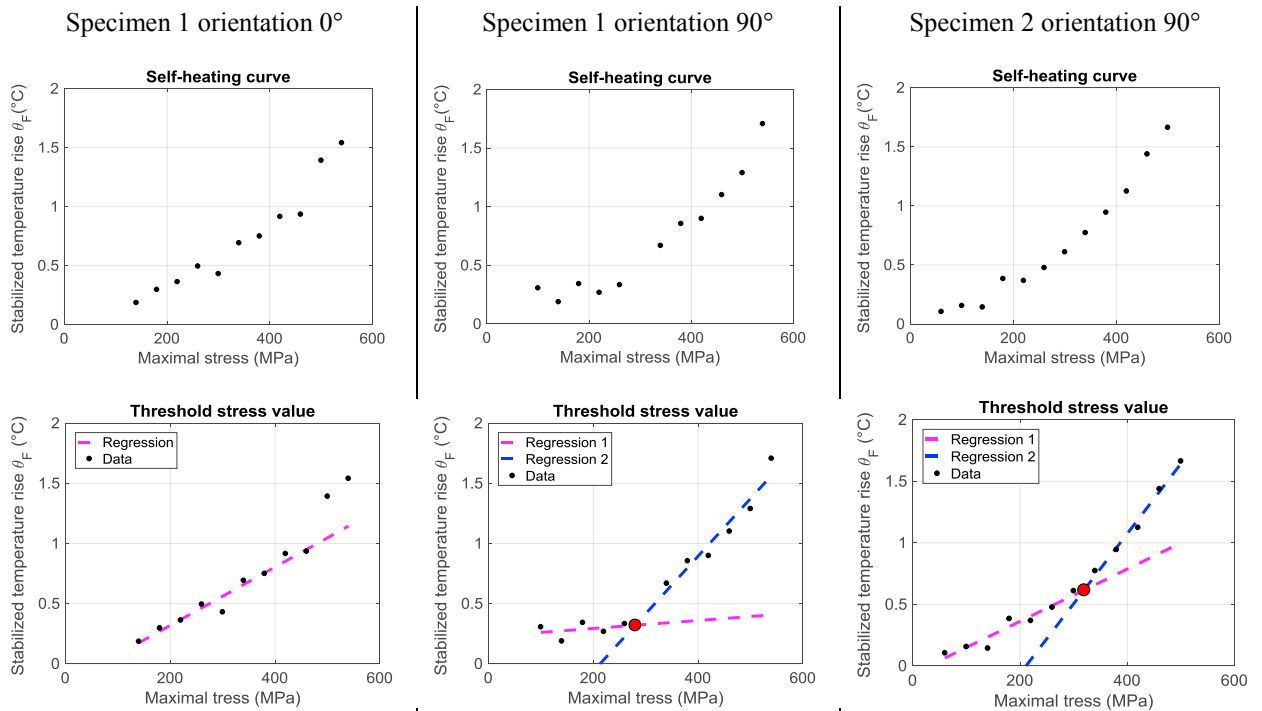


Fig. 9 : Self-heating curves and estimation of the threshold stress values

For both orientations ( $0^\circ$  and  $90^\circ$ ), the self-heating curves show a definite variation of the thermal behavior. However, the precise and reliable identification of a threshold stress value associated with a clear change of heating tendency is not obvious. If the determined values for the  $90^\circ$  specimens seem reliable, the lack of data to define the

second domain for the 0° specimen makes it impossible to properly estimate a stress threshold associated with a change of thermal behavior. Moreover, the values present a high scattering with a large confidence interval, as shown in Table 3.

Table 3 : Threshold stress values for each specimen, and their confidence range

Specimen	Particular stress value	Confidence interval
N°1 at 90°	280 MPa	[193 367] MPa
N°2 at 90°	320 MPa	[268 347] MPa

3.4. Experimental lock-in thermal monitoring at high IR camera frequency

The second chosen approach is to monitor the heating of the sample with a much higher frequency acquisition of 100 images per second in order to analyze the sinusoidal part of the thermal signal, in anti-phase with the mechanical signal (Fig. 10). This lock-in thermography approach had been used by Krapez *et al.* for metallic materials [15].

The same mechanical load was applied, with 12 blocks of cycles, 6,000 cycles per block, with the same load values. For each block of cycles, the infrared camera is triggered to record 10 seconds (about 50 cycles), after 20 and 3,000 mechanical cycles.

Since the load ratio R is constant the stress amplitude grows from one block to another. According to the thermoelastic theory [16], the thermal amplitude  $A_1$  is expected to increase proportionally as long as the material behavior remains in its elastic domain. But during the last steps, a non-linearity of  $A_1(\sigma_{maxi})$  is observed, using the same method of double linear regressions. This change appears at a threshold stress value (Fig. 11).

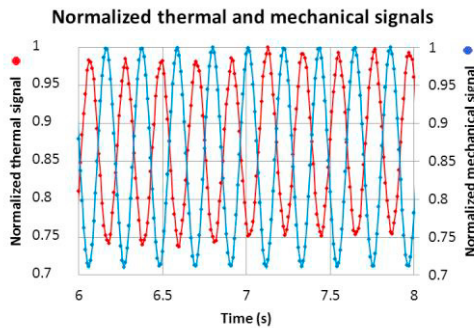


Fig. 10 : Anti-phase variations of the thermal and mechanical signals. Thermal acquisition setup: 100 images per second.

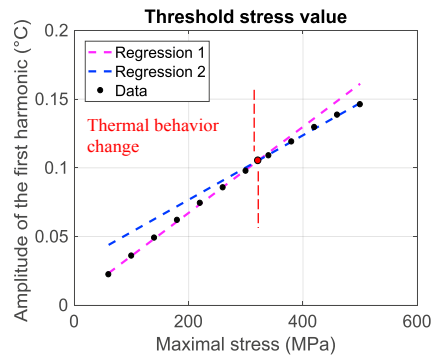


Fig. 11 : Threshold stress value of  $A_1(\sigma_{maxi})$

Table 4 shows the threshold stress values estimated from the  $A_1(\sigma_{maxi})$  curve, for two samples (one of each orientation). It appears that the threshold stress value is the same in both cases, with a relatively low scattering. This means that viscous phenomena and/or damage events altering the thermoelastic behavior are activated at the same stress level. The next step in our study will be to analyze if the fatigue limit is linked to this threshold stress value.

Table 4 : Threshold stress value assessed from the evolution of the first harmonic amplitude, and their confidence range

Specimen	Threshold stress value	Confidence interval
N°2 at 0°	321 MPa	[290 352] MPa
N°3 at 90°	320 MPa	[306 331] MPa



#### 4. Conclusion and outlooks

The first purpose of this paper was to check if the self-heating evolutions described before for thermoset composites are still valid for woven carbon fiber thermoplastic matrix composite materials. It is possible now to answer that the self-heating curves for thermoplastic composites show a definite variation of the thermal behavior. The next step will be to find a procedure to clearly identify the threshold stress value associated with the change of heating behavior. Furthermore, the study of the first harmonic of the thermal signal shows a change of thermoelastic behavior, altering by viscous phenomena and/or damage events. These results will be analyzed, to determine if the fatigue limit is linked to this threshold stress value. Finally, the comparison of thermal behaviors of the material under quasi-static tensile tests and under cyclic loading is still in progress. In particular, the static stress value in orthotropic directions corresponding to the beginning of the non-linearity of the thermal signal and to its minimum will be properly compared to the fatigue limit.

The most immediate follow-up work is to proceed with the analyses of data acquired from the first self-heating tests campaign: acoustic emission, displacement and strain fields may improve the understanding of the link between damage, self-heating and mechanic properties variations. The aim of the study is to achieve an experimental protocol dedicated to a quick and reliable monitoring of the self-heating of thermoplastic composites. On another hand, conventional fatigue tests with millions of cycles will be carried out in collaboration with CETIM to build up Wöhler curves and determine the fatigue limit of our material. A quantitative link will be made between this limit and the self-heating of composite.

#### References

- [1] R. Hamonou, « Contribution à l'analyse du comportement hors plan des assemblages boulonnés : application aux composites thermoplastiques tissés », Ecole Centrale de Nantes (ECN), 2016.
- [2] B. Esmaeilou, « Approche cinétique du comportement en fatigue du Polyamide 66 renforcé par 30% de fibres de verre », Arts et Métiers ParisTech, 2011.
- [3] D. Busca, « Identification du comportement de composites en fatigue bi-axiale », Institut National Polytechnique de Toulouse (INP Toulouse), 2014.
- [4] Z. Boufaïda, « Analyse des propriétés mécaniques de composites taffetas verre/matrice acrylique en relation avec les propriétés d'adhésion des fibres sur la matrice », Institut National Polytechnique de Lorraine, 2015.
- [5] G. Bai, « Evaluation par vibrothermographie de l'endommagement de composites tissés », Université de Bordeaux, 2016.
- [6] J.-L. Chaboche, J. Lemaitre, A. Benallal, et R. Desmorat, *Mécanique des matériaux solides*, 3e éd. Dunod, 2008.
- [7] O. Westphal, « Analyse thermomécanique de l'endommagement en fatigue de stratifiés carbone/époxy: détermination de la limite d'endurance à partir d'essais d'auto-échauffement », Ecole Centrale de Nantes (ECN), 2014.
- [8] M. P. Luong, « Infrared thermographic scanning of fatigue in metals », *Nucl. Eng. Des.*, vol. 158, n° 2-3, p. 363–376, 1995.
- [9] G. La Rosa et A. Risitano, « Thermographic methodology for rapid determination of the fatigue limit of materials and mechanical components », *Int. J. Fatigue*, vol. 22, n° 1, p. 65–73, 2000.
- [10] C. Doudard, « Détermination rapide des propriétés en fatigue à grand nombre de cycles à partir d'essais d'échauffement », Ecole Normale Supérieure de Cachan, 2004.
- [11] C. Colombo, F. Libonati, F. Pezzani, A. Salerno, et L. Vergani, « Fatigue behaviour of a GFRP laminate by thermographic measurements », *Procedia Eng.*, vol. 10, p. 3518–3527, 2011.
- [12] L. Jegou, Y. Marco, V. Le Saux, et S. Calloch, « Fast prediction of the Wöhler curve from heat build-up measurements on Short Fiber Reinforced Plastic », *Int. J. Fatigue*, vol. 47, p. 259–267, févr. 2013.
- [13] L. Gornet, O. Westphal, A. Krasnobrizha, P. Rozycki, C. Peyrac, et F. Lefèbvre, « Détermination rapide de la limite de fatigue d'un tissu carbone à matrice thermoplastique », *Comptes Rendus JNC 19*, 2015.
- [14] L. Vergani, C. Colombo, et F. Libonati, « A review of thermographic techniques for damage investigation in composites », *Frat. Ed. Integrità Strutt.*, vol. 27, 2014.
- [15] J. C. Krapez, D. Pacou, et C. Bertin, « Application of lock-in thermography to rapid evaluation of fatigue limit in metals », *Workshop Adv. Infrared Technol. Appl.*, 1999.
- [16] W.-T. Kim, M.-Y. Choi, Y.-H. Huh, et S.-J. Eom, « Measurement of thermal stress and prediction of fatigue for STS using Lock-in thermography », in *12th A-PCNDT, Asia-Pacific Conference on NDT, Auckland, New Zealand. Auckland, New Zealand*, 2006.